Opto-Electronics Review

journal homepage: https://journals.pan.pl/opelre

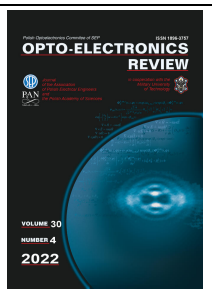

Adaptive and precise peak detection algorithm for fibre Bragg grating using generative adversarial network

Sunil Kumar*, Somnath Sengupta

Department of Electronics and Communication Engineering, Birla Institute of Technology, Mesra, Ranchi, Jharkhand, India

Article info

Article history:
Received 27 Aug. 2022
Received in revised form 31 Oct. 2022
Accepted 28 Nov. 2022
Available on-line 27 Dec. 2022

Keywords:
Fibre Bragg grating; generative model; discriminative model; loss function.

Abstract

An adaptive and precise peak wavelength detection algorithm for fibre Bragg grating using generative adversarial network is proposed. The algorithm consists of generative model and discriminative model. The generative model generates a synthetic signal and is sampled for training using a deep neural network. The discriminative model predicts the real fibre Bragg grating signal by the calculation of the loss functions. The maxima of loss function of the discriminative signal and the minima of loss function of the generative signal are matched and the desired peak wavelength of fibre Bragg grating is determined. The proposed algorithm is verified theoretically and experimentally for a single fibre Bragg grating peak. The accuracy has been obtained as ±0.2 pm. The proposed algorithm is adaptive in the sense that any random fibre Bragg grating peak can be identified within a short wavelength range.

1. Introduction

Fibre Bragg grating (FBG) is an optical fibre sensor that has wide applications to measure physical parameters such as temperature, strain, torque, fault detection in transmission lines, humidity, magnetic field, etc [1]. The FBGs can be used for static, as well as dynamic sensing with high repeatability and in hard conditions. Due to its small size, longer life, and less maintenance, it has a superior sensing capability over traditional electronic sensors. It has a better capability to be immune to the electromagnetic interference [2]. FBGs have been used in different fields of industries, including aerospace, structural health monitoring, micro seismic wave detection, inclination measurement, and load measurement systems [3–7]. The reflected spectral data of FBG is generally measured by an optical spectrum analyser (OSA), but it is not suitable for a dynamic peak measurement. To effectively measure the FBG peak, the spectral data is collected, and some suitable peak detection algorithm is generally applied through a computer device. Several peak detection techniques have been developed, e.g., polynomial curve fitting [8], direct method [9], centroid detection method [10], a non-linear Gaussian method [11], etc., for a single FBG peak, and matched filtering technique [12], Hilbert transforms [13], cross-correlation and Hilbert transform [14], self-adaptive [15], invariant moment retrieval [16], etc., for a multiple FBG peak detection. However, these techniques are not dynamic and have a slow time response. However, to improve the speed of peak detection, different machine learning techniques have been developed such as support vector machine (SVM) [17], decision tree with SVM [18], extreme learning machine [19], K-nearest neighbours' algorithm [20], deep learning network [21], feature extraction support vector machine (FE-SVM) [22], deep convolutional neural network [23], etc. In these techniques, however, there are some drawbacks regarding mean square error and speed, etc.

In this paper, the peak detection algorithm for FBG using a generative adversarial network is proposed.

The algorithm consists of generative model and discriminative model. The generative model generates a synthetic signal and is sampled for training using a deep neural network. The discriminative model predicts the real FBG signal by the calculation of the loss function. The maxima of loss function of the discriminative signal and the minima of loss function of the generative signal are matched and the desired peak wavelength of FBG is

*Corresponding author at: skp.narayan@gmail.com

https://doi.org/10.24425/opelre.2022.144227
1896-3757/ Association of Polish Electrical Engineers (SEP) and Polish Academic of Sciences (PAS). Published by PAS

determined. The proposed algorithm is verified theoretically and experimentally for a single FBG peak.

2. Theory of algorithm

FBG has reflective characteristics at a particular wavelength when a monochromatic light source is incident on it. The reflected wavelength is written as

$$\lambda_B = 2\Lambda n_{eff}, \tag{1}$$

where λ_B is the Bragg wavelength, Λ is the grating period, and n_{eff} is the effective refractive index of the core mode of the optical fibre. The change in Bragg wavelength is proportional to the change in the physical parameters as temperature, strain, etc. The proposed FBG peak detection algorithm using a generative adversarial network (GAN) based machine learning is described in Fig. 1. The GAN is based on generative model (GM) and discriminative model (DM). The function of the GM is to generate a synthetic signal as the FBG signal. In the GM, the gaussian function is used to generate a synthetic signal in this proposed technique. Also, a model signal is assumed, the wavelength range of which is considered as the same as the FBG signal. Next, the generated model signal is sampled and trained using a deep neural network (DNN), for fast processing. After sampling and training, the generator model signal is passed through the discriminator model. The FBG or real signal is also passed through discriminator model for sampling. The DM discriminates the real signal and synthetic signal using DNN by calculating the loss function of the discriminated real signal and generated signal. The loss function of the discriminated signal is maximized, and the loss functions of the generated signal is minimized at a specific wavelength which is the desired peak wavelength.

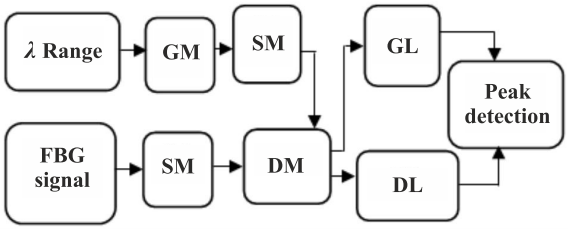

Fig. 1. Block diagram of the GAN model: SM – sampling, GL – generator loss, DL – discriminator loss.

The GAN training model using DNN for the peak detection algorithm of FBG is illustrated in Fig. 2. The training model is classified by two states, the first state is a reference signal generated by GM and the second state is the FBG signal collection. The GM and DM are trained separately, and then the respective signals are sampled at different levels. The levels as $I_1, \ldots, I_k$ are for generated signal and $R_1, \ldots, R_k$ are for reflectivity spectrum of FBG. The sampled data of both the generated and the FBG signals are mapped into discriminator levels.
The training of GM and DM in GAN is described as:

a) discriminator model training

As mentioned, the GAN model includes the generator model and discriminator model. During the GAN training, only one model is trained at a time, and the other model is

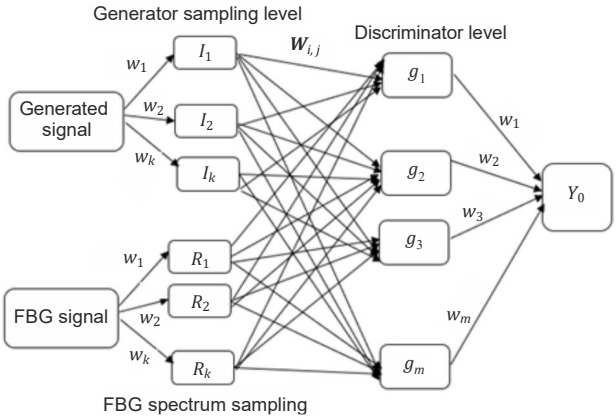

Fig. 2. DNN structure for FBG peak detection.

kept as untrained. During the training of DM, the GM is assumed as untrained or fixed. Using the cross entropy, as given in (3), the loss function is derived as

$$F(D(\lambda), G(\lambda)) = E(\log(D(\lambda)) + E(\log(1 - G(\lambda)), \tag{2}$$

where $\log(D(\lambda))$ is the loss function of the discriminator model and $\log(1 - G(\lambda))$ is the loss function of the generator model.

The goal of discriminator is to maximize the loss function $F(R(\lambda), I(\lambda))$ through differentiation with respect to $D(\lambda)$ to find the optimal value of discriminator as

$$D^*(\lambda) = \frac{P_{R(\lambda)}}{P_{R(\lambda)} + P_{I(\lambda)}}, \tag{3}$$

where $P_{R(\lambda)}$ is the probability estimation of the real signal and $P_{g(\lambda)}$ is the probability estimation of the generated signal. To optimize $D^*(\lambda)$, $P_{R(\lambda)}$ should be maximum and would approach 1, $P_{I(\lambda)}$ is minimum at a given position point.

b) generator model training

To train the generator model, the discriminator model was held fixed and a training process was using a mathematical expression, given as

$$F(G(\lambda), D^*(\lambda)) = E(\log(D^*(\lambda)) + E(\log(1 - D^*(\lambda)). \tag{4}$$

By combining (3) and (4), it can be written:

$$F(G(\lambda), D^*(\lambda)) = E\left[\log\frac{P_{R(\lambda)}}{P_{R(\lambda)} + P_{I(\lambda)}}\right] + E\left[\log\frac{P_{g(\lambda)}}{P_{R(\lambda)} + P_{I(\lambda)}}\right]. \tag{5}$$

By using the Kullback-Leibler (KL) concept of divergence, in (5), $F(G(\lambda), D^*(\lambda))$ is minimum when $P_{g(\lambda)}$ is minimum, say equal to zero. Thus, the minimum of $P_{g(\lambda)}$ means that the true signal is identified by calculating the loss functions of the generated signal and the real FBG signal. The loss function is maximum for the discriminated signal and minimum for the generated signal at a specific wavelength.

The mathematical model of the DNN mentioned in Fig. 2, is explained by (6) to (10). Equation (6) calculates the min-max loss function using the discriminator levels $g_1, \ldots, g_m$ and the comparison of weights $w_1, \ldots, w_m$. Equation (7) calculates the different discriminator levels $g_1, \ldots, g_m$ using the convolution function $f(I_j, R_j)$ and the weight factor $W_{i,j} (i = 1, \ldots, k, j = 1, \ldots, m)$. The function $f(I_j, R_j)$ is nothing but the convolution of sampled versions of the generated signal and the FBG signal, which is explained in (8). The weight factor $W_{i,j}$ used in (7) is updated each time until the minima of the generated signal and maxima of the discriminated signal arrives at the same point. This is achieved by finding the zero points of the differentiation of the function $f(I_j, R_j)$ with respect to λ and adding the old weight factor. This is expressed in (9). Similarly, the weight factor w_i used in (10) is updated according to the expression given in (10). After training and peak matching of the generated signal and the discriminated signal, the loss functions of discriminator model signal and of generator model signal are calculated using (11), and using (12), the desired peak wavelength as λ_B is determined.

$$Y_0 = \sum_{i=1}^{m} g_i w_i \tag{6}$$

$$\sum_{i=1}^{m} g_i = \sum_{j=1}^{k} f(I_j, R_j) W_{i,j} \tag{7}$$

$$f(I_j, R_j) = (w_k I_j) \cdot (w_k R_j) \tag{8}$$

$$Wi, j_{new} = Wi, j_{old} + \text{zero\_P}\left(\frac{df(I_j, R_j)}{d\lambda}\right) \tag{9}$$

$$w_i = \max(W_{new}) + \text{zero\_P}\left(\frac{d(g)}{d\lambda}\right) \tag{10}$$

$$L = \text{Loss}\left(\sum_{i=1}^{m} g_i\right) \tag{11}$$

$$\frac{dL}{d\lambda} = 0 \tag{12}$$

3. Simulation of the FBG peak detection algorithm using GAN

The proposed FBG peak detection algorithm using GAN has been simulated for a single FBG peak. The coupled-mode theory [16] is used and the simulated reflected spectrum for FBG is represented as

$$R_s(\lambda) = \frac{\sinh^2\left(\sqrt{k^2 - s^2}\mathrm{L}\right)}{\cosh^2\left(\sqrt{k^2 - s^2}\mathrm{L}\right) - \frac{s^2}{k^2}}, \tag{13}$$

$$k = \frac{2\pi}{\lambda} \cdot v \cdot dn_{eff}, \quad d = 2n\pi\left(\frac{1}{\lambda} - \frac{1}{\lambda_B}\right),$$
$$S = \frac{2\pi}{\lambda} \cdot dn_{eff} \quad \text{and} \quad s = S + d,$$

where k is the ac-coupling factor, S is the dc-coupling factor, d is the detuning factor. A single FBG peak within the wavelength range from 1542 nm to 1544 nm with a central peak at 1543 nm was considered. The reflectivity of a single FBG spectrum is calculated and plotted in Fig. 3(a). According the GAN structure, the gaussian model is used as a generator model to generate a synthetic signal having a similar shape to the FBG reflected spectrum and written as

$$I(\lambda) = ae^{\frac{(\lambda - \lambda_t)^2}{2D_\lambda^2}}, \tag{14}$$

where 'a' is the height of the generated signal, D_λ is the bandwidth deviation, λ_t is the central peak of the generated signal. It is plotted in Fig. 3(b).

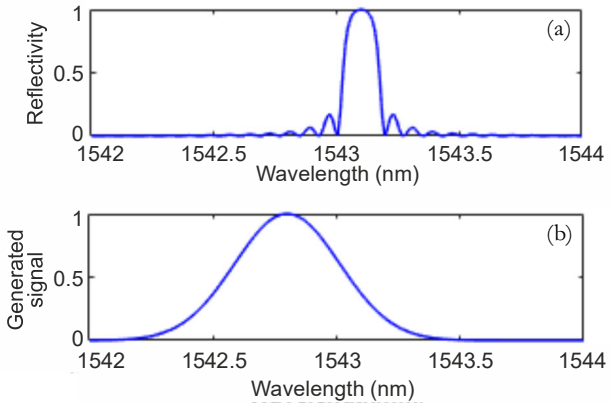

Fig. 3. Reflectivity of simulated FBG spectrum (a). Generated synthetic signal (b).

The data for training is generated by the reflectivity formula, which is derived from the coupled-mode theory using simulation, and the proposed algorithm is applied to the simulation data.

According to the algorithm, λ_t will be changed and matched with the peak wavelength of FBG by DNN training. The corresponding generated signal and the FBG signal are plotted in Fig. 4. The regression analysis is performed by calculating the regression (R) value, which is plotted in Fig. 5. To analyse the regression, the DNN is used for training, testing, and validation. 70% of the FBG simulated data is used for training and 30% of the simulated data is used for testing. The performances of training and testing are calculated in terms of R-values as 0.9999 and 0.99983, respectively. The overall performance of regression is calculated as 0.99988 and it can be seen that the regression value is high when the peak of the FBG spectrum and the generated signal are matched. If the regression value is low, then the peaks are not matched properly. The high R-value means that the mean square error (MSE) is very low, which is calculated as 0.00001147

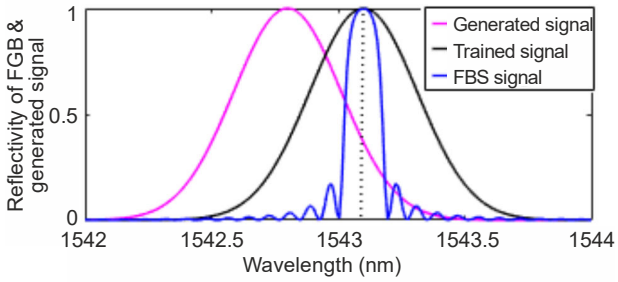

Fig. 4. Trained signal of the simulated FBG spectrum and the generated signal for peak matching using GAN.

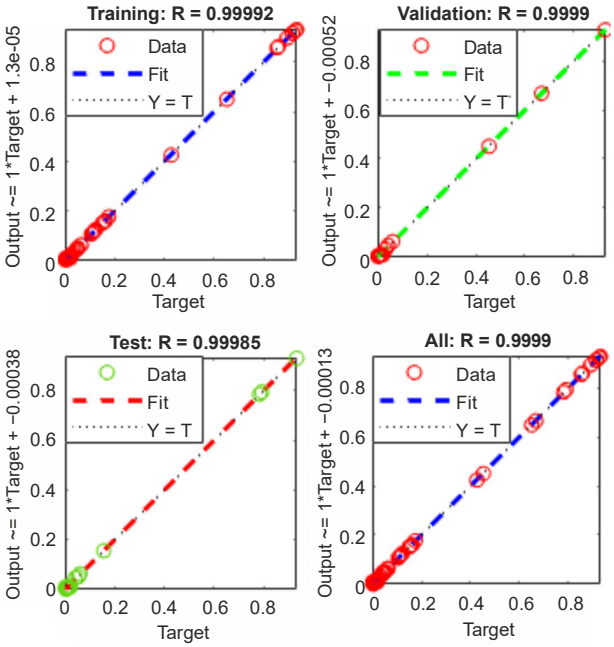

Fig. 5. Regression analysis of training, testing, validation, and overall training performance of GAN.

at epoch 62, as plotted in Fig. 6. After 62 epochs, the training, testing, and validation lines cross the line of the best set with very less error. The performance of training is plotted in Fig. 7, and it is found that the best validation performance is 0.00001147 at epoch 62. The low validation performance means the MSE is very low and nearly equal to zero.

After regression, the loss function of discriminated signal and the loss function of generated signal is calculated and expressed as

$$L_g = \log\big(1 - I(\lambda)\big), \tag{15}$$

$$L_d = \log\big(R(\lambda)\big). \tag{16}$$

The maxima of the loss function of the discriminated signal and the minima of the loss function of the generated signal lie at the same wavelength as 1543.1 nm for the assumed single FBG plotted in Fig. 8. The derivatives of the loss function are equal to zero to find the exact peak wavelength of FBG. The simulated result was verified experimentally and explained in section 4.

4. Experiment setup and results

The proposed algorithm for peak detection of FBG using GAN is performed experimentally. The experimental setup is mentioned in Fig. 9. The light is coupled into the FBG from a broadband light source through a Y-coupler. At the port-1 of the Y-coupler, the broadband light source is entered and emerges at port-2 of the Y-coupler. The emerged light on port-2 is incident on a single FBG with a wavelength range from 1548 nm to 1552 nm with a central peak at 1549.5 nm. The reflected spectrum of FBG is fed back into port-2 of the Y-coupler and emerges at port-3. The reflected spectrum data at port-3 is collected by a computer device from an optical spectrum analyser through a GPIB cable.

The experimental data are generated through the experimental setup which is mentioned in Fig. 9. The

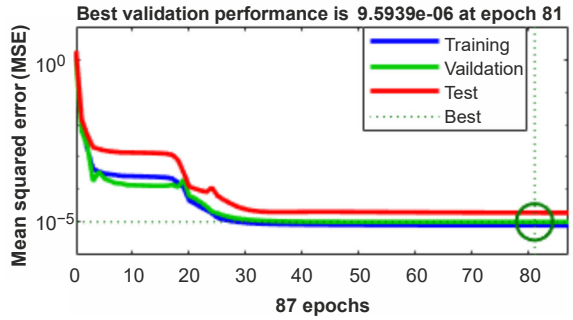

Fig. 6. Training performance analysis.

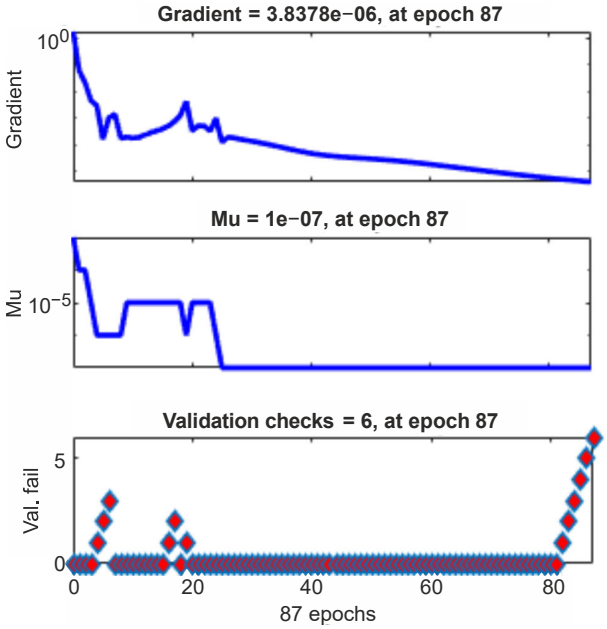

Fig. 7. Training state of regression.

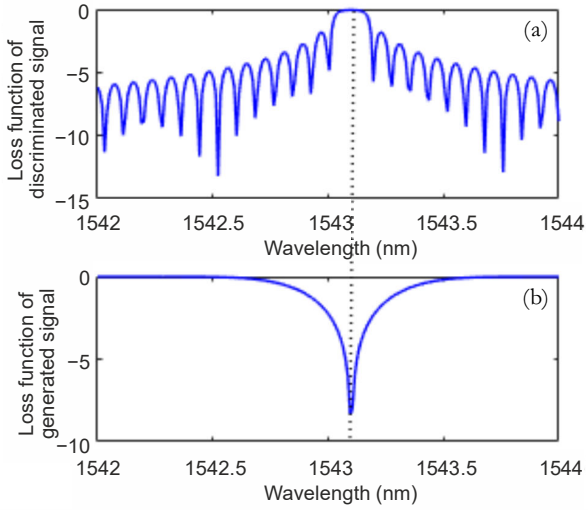

Fig. 8. Loss function of discriminated signal (a), loss function of generated signal (b).

proposed algorithm is applied to the collected experimental data. The discriminator model trains the generated sampled data and the real FBG sampled data. The average mean value, variance and the loss function are calculated in each training state and the desired peak wavelength is determined by the discriminator using the loss function.

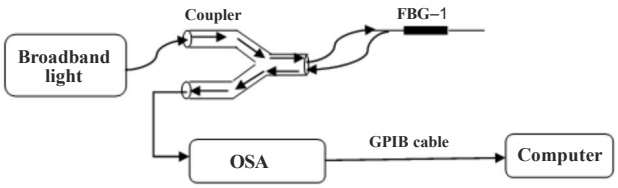

Fig. 9. Experimental setup for FBG spectral data.

The normalized FBG reflectivity spectrum is plotted in Fig. 10 and is sampled for training using DNN. The generated synthetic signal is also sampled and trained using DNN. The trained FBG signal and the generated signal are analysed by regression process. The regression analysis shows the characteristics of the training, testing, and validation which are performed efficiently and plotted in Fig. 11. It is seen that the regression value approaches 1 with a value of 0.999 and the performance of validation or MSE is very low, close to zero, as shown in Fig. 12. This indicates that the loss function of the discriminated signal would be maximum. Furthermore, the min-max of the loss functions of the discriminated signal and the generated signal were analysed by the training state as plotted in Fig. 13. It can be seen that the μ-parameter is very low as e^{-7} with a low gradient value of 0.000002 at epoch 18.

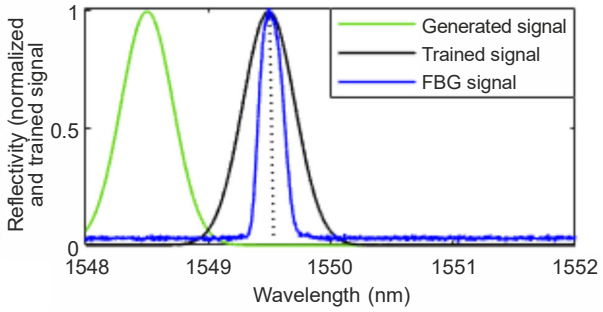

Fig. 10. Trained signal of the experimental FBG signal and generated signal for peak matching using GAN in the experimental data.

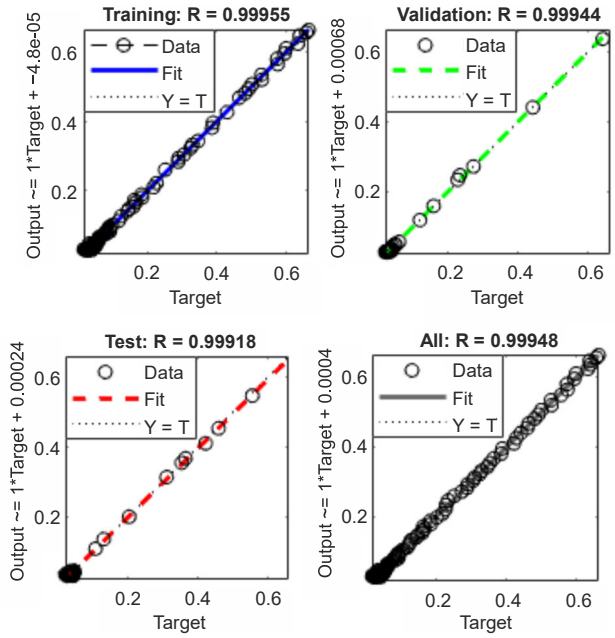

Fig. 11. Regression analysis of training, testing, and validation of the experimental data.

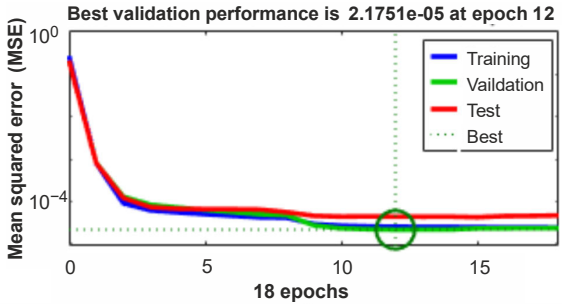

Fig. 12. Performance analysis of trained GAN.

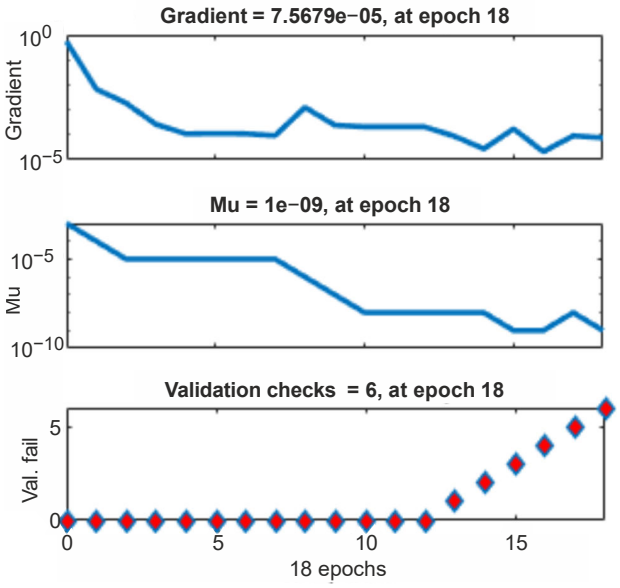

Fig. 13. Training state analysis using DNN-GAN.

During the regression it is found that the R-value is high, it means that the peak of the FBG signal and the generated signal are matched, as it was previously explained in Fig. 10. The matched signal is realised by the discriminator by calculating the loss function of the generated signal and the discriminated real signal. As a result, the loss function of the real signal is maximum and that of the generated signal is minimum at a particular wavelength which is the desired peak wavelength. The equi-point of both positions of loss functions is calculated as 1549.5002 nm and plotted in Fig. 14. The measured peak wavelength is closest to the central peak of the FBG used in the experiment as 1549.5000 nm, and it can be seen that the error is very small like 0.2 pm. Thus, the proposed peak detection algorithm for FBG using GAN is experimentally verified with good accuracy.

In the proposed method of detecting FBG peaks using GAN, a statistical analysis method is applied after training the model to find the p-value and confidence interval (CI) using the expression as:

$$CI_U = \text{mean}(X) + t \cdot \frac{s}{\text{square}(n)}, \tag{17}$$

$$CI_L = \text{mean}(X) - t \cdot \frac{s}{\text{square}(n)}, \tag{18}$$

$$p\text{-value} = 2 \cdot \left(1 - cdf(t_\lambda)\right), \tag{19}$$

where, CI_U is the upper CI value and CI_L is the lower CI value, $cdf\ (t_\lambda)$ is the cumulative distribution function of test statics.

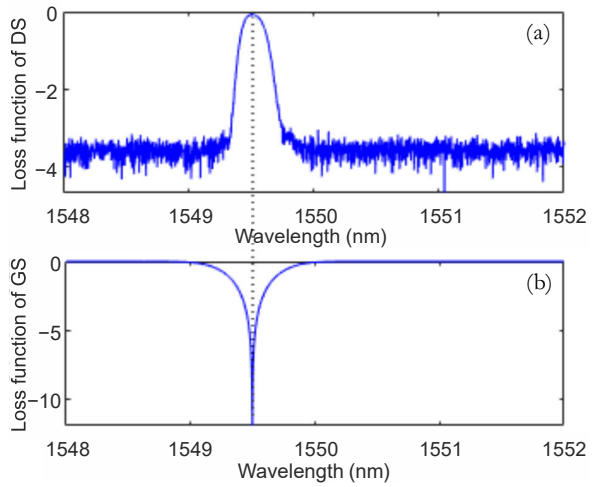

Fig. 14. Loss function of the trained network of the discriminated signal and the generated signal when matching the position of the maxima of the discriminated signal (a) and the minima position of the generated signal (b).

Using (17), (18), and (19), the p-value is calculated as $1.0296 \cdot 10^{-77}$ and the CI is [0.0707–0.0865]. Here, the p-value is less than the significance value of 0.05, this means that the hypothesis is more significant and there is a 99.9 chance that a specific interval contains the true peak wavelength. Thus, based on the analysis, it can be said that the proposed FBG peak detection method has good accuracy.

A comparison of different peak detection methods is given in Table 1.

Table 1.
Comparison of different peak detection methods.

Ref. no.	FGB peak detection methods based on:	3-dB bandwidth of the considered FBG signal	Mean	MSE
[13]	Hilbert transform	0.212 nm	5.80 pm	–
[16]	Invariants moment interval	0.3 nm	0.19 pm	0.5 pm
[18]	Machine learning techniques for liquid level estimation	0.5 nm	–	3.58 pm
[22]	Deep learning algorithms for FBG	–	7.8 pm	8.48 pm
[24]	Machine learning	–	–	0.258 pm
–	GAN (present work)	0.3 nm	0.008 pm	0.20 pm

The different peak detection techniques are compared with the proposed FBG peak detection techniques using GAN-based machine learning and the authors found the mean value as 0.008 pm and the MSE value of 0.20 pm which are the lowest compared with other methods.

5. Conclusions

A peak detection algorithm for FBG using GAN-based machine learning is proposed. It has been verified both theoretically and experimentally. In GAN, a random gaussian spectral signal is considered as the GM and the real FBG signal is used in the discriminator model. The loss functions are calculated for the generated signal and discriminated signal. The peak of the generated signal matches with the peak of the real signal after training for at least 1 or 2 epochs. The proposed algorithm is very much suitable for a dynamic change of the FBG peak but limited in the short wavelength range. For the long wavelength range, it would require, however, more epochs, i.e., around 30 epochs. The proposed algorithm can be extended for multi-FBG peak detection with good accuracy and can even be suitably applied for overlapped peaks.

Authors' statement

In the manuscript "Adaptive and precise peak detection algorithm for fibre Bragg grating using generative adversarial network", the authors have contributed as follows: S.K carried out the study of all the parameters which are used in the proposed peak detection technique, the design of peak detection algorithm, and the result analysis. Drafting and writing of the manuscript was carried out by S.S.

References

[1] Chen, G. Y.& Brambilla, G. Optical Microfiber Physical Sensors. in *Optical Fiber Sensors: Advanced Techniques and Applications* (ed. Rajan, G.) chapter 8 (CRC Press, 2017).

[2] Fiber optic bio and chemical sensors. in *Fiber optic sensors* (eds. Yin, Sh., Ruffin, P. B. & Yu, F. T. S.) 435–457 (CRC Press, 2008).

[3] Ma, Z. & Chen, X. Fiber Bragg gratings sensors for aircraft wing shape measurement: Recent applications and technical analysis. *Sensors* **19**, 55 (2018). https://doi.org/10.3390/s19010055

[4] Jinachandran, S. *et al.* Fabrication and characterization of a magnetized metal-encapsulated FBG sensor for structural health monitoring. *IEEE Sensor J.* **18**, 8739–8746 (2018). https://doi.org/10.1109/JSEN.2018.2866803

[5] Gautam, A., Kumar, A. & Priya, V. Microseismic wave detection in coal mines using differential optical power measurement. *Opt. Eng.* **58** 056111 (2019). https://doi.org/10.1117/1.OE.58.5.056111

[6] Kinjalk, K., Kumar, A. & Gautam, A. High-resolution FBG-based inclination sensor using eigen decomposition of reflection spectrum. *IEEE Trans. Instrum. Meas*. **69**, 9124–9131 (2020). https://doi.org/10.1109/TIM.2020.2999116

[7] Vickers, N. J. Animal communication: when I'm calling you, will you answer too. *Curr. Biol*. **27**, R713–R715 (2017). https://doi.org/10.1016/j.cub.2017.05.064

[8] An, Y., Wang, X., Qu, Zh., Liao, T. & Nan, Zh. Fiber Bragg grating temperature calibration based on BP neural network. *Optik* **172**, 753–759 (2018). https://doi.org/10.1016/j.ijleo.2018.07.064

[9] Chen, Z.-J. *et al*. Optimization and comparison of the peak-detection algorithms for the reflection spectrum of fiber Bragg grating. *Acta Photon. Sin.* **44**, 1112001 (2015). [in Chinese]

[10] Trita, A. *et al*. Simultaneous interrogation of multiple fiber Bragg grating sensors using an arrayed Waveguide grating filter fabricated in SOI platform. *IEEE Photon. J.* **7**, 1–11 (2015). https://doi.org/10.1109/JPHOT.2015.2499546

[11] Junfeng, J. *et al*. Distortion-tolerated high speed FBG demodulation method using temporal response of high-gain photodetector. *Opt. Fiber Technol*. **45**, 399–404 (2018). https://doi.org/10.1016/j.yofte.2018.08.019

[12] Kumar, S. *et al*. Efficient detection of multiple FBG wavelength peaks using matched filtering technique. *Opt. Quantum Electron.* **54**, 1–14 (2022). https://doi.org/10.1007/s11082-021-03460-3

[13] Liu, F. *et al*. Multi-peak detection algorithm based on the Hilbert transform for optical FBG sensing. *Opt. Fiber Technol*. **45**, 47–52 (2018). https://doi.org/10.1016/j.yofte.2018.06.003

[14] Theodosiou, A. *et al*. Accurate and fast demodulation algorithm for multipeak FBG reflection spectra using a combination of cross-correlation and Hilbert transform. *J. Light. Technol*. **35**, 3956–3962 (2017). https://doi.org/10.1109/JLT.2017.2723945

[15] Chen, Y., Yang, K. & Liu, H.-L. Self-adaptive multi-peak detection algorithm for FBG sensing signal. *IEEE Sensors J*. **16** 2658–2665 (2016). https://doi.org/10.1109/JSEN.2016.2516038

[16] Guo, Y., Yu, C., Yi, N. & Wu, H. Accurate demodulation algorithm for multi-peak FBG sensor based on invariant moments retrieval. *Opt. Fiber Technol*. **54**, 102129 (2020). https://doi.org/10.1016/j.yofte.2019.102129

[17] Li, Hong, *et al*. Recognition and classification of FBG reflection spectrum under non-uniform field based on support vector machine. *Opt. Fiber Technol*. **60**, 102371 (2020). https://doi.org/10.1016/j.yofte.2020.102371

[18] Nascimento, K. P., Frizera-Neto, A., Marques, C. & Leal-Junior, A. G. Machine learning techniques for liquid level estimation using FBG temperature sensor array. *Opt. Fiber Technol*. **65**, 102612 (2021). https://doi.org/10.1016/j.yofte.2021.102612

[19] Jiang, H., Cheng, J. & Liu, T. Wavelength detection in spectrally overlapped FBG sensor network using extreme learning machine. *IEEE Photon. Technol. Lett.* **26**, 2031–2034 (2014). https://doi.org/10.1109/LPT.2014.2345062

[20] Leal-Junior, A. G.A machine learning approach for simultaneous measurement of magnetic field position and intensity with fiber Bragg grating and magnetorheological fluid. *Opt. Fiber Technol.* **56**, 102184 (2020). https://doi.org/10.1016/j.yofte.2020.102184

[21] Ee, Y.-J. *et al*. Lithium-ion battery state of charge (SoC) estimation with non-electrical parameter using uniform fiber Bragg grating (FBG). *J. Energy Storage* **40**, 102704 (2021). https://doi.org/10.1016/j.est.2021.102704

[22] Kokhanovskiy, A., Shabalov, N., Dostovalov, A. & Wolf, A. Highly dense FBG temperature sensor assisted with deep learning algorithms. *Sensors* **21**, 6188 (2021). https://doi.org/10.3390/s21186188

[23] Cao, Z., Zhang, S., Liu, Z. & Li, Z. Spectral demodulation of fiber Bragg grating sensor based on deep convolutional neural networks. *J. Light Technol*. **40**, 4429–4435 (2022). https://doi.org/10.1109/JLT.2022.3155253

[24] Manie, Y. Ch. *et al*. Using a machine learning algorithm integrated with data de-noising techniques to optimize the multipoint sensor network. *Sensors* **20**, 1070, (2020). https://doi.org/10.3390/s20041070